Chemico-Biological Interactions 374 (2023) 110396

Contents lists available at ScienceDirect

Chemico-Biological Interactions

journal homepage: www.elsevier.com/locate/chembioint

Research paper

Quantum dots are time bomb: Multiscale toxicological study

Denis Kuznetsov [a,*], Dmitriy Krylsky [b], Sergey Dezhurov [b], Alexei Grachev [c], Valery Neschisliaev [d], Ekaterina Orlova [d], Anastasiia Kuznetsova [d]

[a] G.N. Gabrichevsky Scientific and Research Institute of Epidemiology and Microbiology, 10, Admirala Makarova str., Moscow, 125212, Russia
[b] Research Institute of Applied Acoustics, Center of High Technologies, 7A, 9 Maya, Dubna, 141980, Russia
[c] Institute of Carcinogenesis, Cancer Research Center of N.N. Blokhin, Kashirskoe sh. 24, Moscow, 115478, Russia
[d] Perm State Pharmaceutical Academy, Polevaya str. 2, 614000, Perm, Russia

ARTICLE INFO

Handling Editor: Brian S Cummings

Keywords:
Quantum dots
Toxicity
Chronic inflammation
Target organs

ABSTRACT

The use of quantum dots has spread widely into many applications. Works on the study of quantum dots on living organisms have had conflicting results on toxicity. There are no full-scale long-term toxicological studies with multiple administration of quantum dots. Understanding the toxicity of quantum dots is still limited. Here we present data on the effects of quantum dots on animals. In this work for the first time, it is shown that at a single administration of quantum dots in the body they have moderate species-specific toxicity, but repeated administration of quantum dots for 14 days even in the amount of 0.5 mg/kg leads to a delayed not completely irreversible hematotoxic effect, delayed irreversible disorders of barrier function of the liver, irreversible nephrotoxic effect, and to pathological changes in the thymus, kidneys and spleen. Administration of quantum dots in the amount of 2.5 mg/kg for 14 days leads to irreversible changes in the lungs, liver, spleen, kidneys and thyroid gland. This phenomenon is based on immunological reactions. On the one hand, these data confirm that quantum dots at a single administration can show relatively low toxicity. On the other hand, they cause to a delayed irreversible organ and tissue damage when repeatedly administered to the body even in small quantities. This study demonstrates that quantum dots are not as low in toxicity as previously thought to be and pose a serious risk when entering living organisms. Detecting and treating poisoning using standard methods of diagnosis and treatment of heavy metal poisoning may not be effective. This study demonstrates that toxic effects of quantum dots on a living body are quite complex and cannot be generalized based on previously reported assumptions.

1. Introduction

Nanotechnology and nanoscience have become a lifesaver for the problems of today's generation, and have been reported in many systems [1–5]. Quantum dots (QDs) are semiconductor nanocrystals, which are the most important group of nanomaterials. Because of their unique optical properties, research in the development of various biomedical applications has been one of the most popular in the last 10 years. Most of the efforts of scientists have been aimed at the configuration of properties of nanocrystals, reducing their size, and improving their optical characteristics [6–23]. There are various types of quantum dots: CdS, PbS, InP, graphene QDs, etc. [13,20,24–28]. As before, cadmium QDs outperform all others by quantum yield, half-height fluorescence peak width (FWHM), photostability and ability to set a fluorescence peak in a wide range (390–800 nm), as well as by the cost and ease of synthesis [14,23,24,29].

Recent reviews show that various cadmium-based QDs have IC50 values ranging from 19 to 696 μg/ml, ZnO-based QDs from 5.75 to 125 μg/ml, Ag2S-based from 23.2 to 1.361 μg/ml, AgInS2-based from 57.523 μg/ml, CuO-based from 7.4 μg/ml, graphene-based QDs from 24.81 to 2.000 μg/ml [30,31]. We obtained QDs. During the process toxicity was reduced due to obtaining more chemically stable nanocrystals and their encapsulation in a biocompatible shell of polyvinylpyrrolidone and maleic acid. We investigated the cytotoxicity of QDs and their conjugates with antibodies, their fragments, and BSA on various cell types. IC50 values ranging from 324 to 776 μg/ml were calculated. Meanwhile, in the due course of the experiment the IC50 for free QDs was not reached (IC50 > 1000 μg/ml). The results of all these studies show considerable variation in the cytotoxicity of QDs of different structures and compositions and can range from "Potentially very toxic" (IC50 < 10 μg/ml) to "Potentially non-toxic" (IC50 > 1000

* Corresponding author.
E-mail address: denis.pfa@gmail.com (D. Kuznetsov).

https://doi.org/10.1016/j.cbi.2023.110396
Received 9 December 2022; Received in revised form 3 February 2023; Accepted 7 February 2023
Available online 9 February 2023

Abbreviation's list

EDX – energy-dispersive X-ray spectroscopy
FWHM – half-height fluorescence peak width
IC50 – half maximal inhibitory concentration
IV – intravenous
LD50 – median lethal dose
RES – reticuloendothelial syste
ROS – reactive oxygen species
QDs – quantum dots

μg/ml).

In *in vivo* studies, an extensive number of works focused on the toxicity of various QDs at single administration. These studies showed weak or no toxic effects of QDs on animals, mainly the effect was in the form of weight loss in animals [33–35]. At the same time, a number of publications shows that even with long-term observation of animals no toxic effects from a single administration of QDs were detected, including the administration of cadmium QDs [36–42]. Such data can cause a so called "*illusory correlation*" that QDs have a significant potential for the development of diagnostic and theranostic drugs. Drug safety is the key parameter. To determine the prospects for this area we carefully planned and conducted research to study the toxicity of cadmium QDs encapsulated in a copolymer shell. This allowed us to obtain a wide range of new data giving an insight into the main toxic effects and target organs during single and multiple IV administration of QDs into the body.

2. Materials and methods

2.1. Fluorescent nanoparticles and their conjugates

Fluorescent CdTeSe/CdS/CdZnS/ZnS nanocrystals were obtained using the procedure described in Ref. [43]. Quantum dots were encapsulated in a copolymer of N-vinylpyrrolidone and acrylic acid. Purification was performed by gel filtration on a Superosa 6 column. The subject was a sterile dispersion of QDs 0.2%, excipients human albumin 100 mg, sodium hydrophosphate 2.8 mg, and water for injection, up to 2 ml, pH 7. Sterilization was performed by sterilizing filtration through a 0.22 μm membrane. The product was characterized by HAADF-STEM, fluorometry, spectrophotometry, and DLS. The research methods and results are presented in Supplementary materials (Fig. S1).

2.2. Animals

To reduce the number of animals used, all work was performed on female animals. F1 mice (CBAxC57Bl/6j), age 7–9 weeks, body weight 20.2 ± 1.3 g; Wistar Outbred rats, age 10–11 weeks, body weight 200 ± 9 were used to study toxicity at a single administration. For the study of toxicity at multiple administrations, we used noninbred rats, 8–10 weeks old, 143.8 ± 5.4 g (Scientific Center for Biomedical Technologies, FMBA (Andreevka Branch)). Animals without signs of health abnormalities were randomly grouped by body weight so that individual body weight fell within the range of ±20% of the mean value of the index for each sex. Each animal was assigned an individual number. The cage label indicated the group, animal numbers, study code, study supervisor's name, doses, and dates of administration of the test substance.

2.3. Study of the toxicity for single IV administration

To determine the toxic effects of QDs during a single intravenous (slow; injection rate 0.5 mL/min) injection into mice, nanoparticle dispersion doses were examined: 10.0, 20.0, 30.0, 40.0, 45.0, and 50.0 mg/kg. When studying the toxicity of QDs on rats, the study of the following doses was conducted: when injected IV: 5.0, 10.0 and 20.0 mg/kg. Control animals were injected with 0.9% NaCl (negative control). The day of administration of QDs and the control substance was considered as day 0. The animals soon showed clinical signs of intoxication, animal death from toxicity, the timing of animal death, changes in body weight of mice and rats, as well as feed and water consumption.

2.4. Determination of toxicity by repeated IV administration

A detailed description of the experiment is given in Supplementary materials. Rats were administered by QDs for 14 days, once a day IV. Control animals were given 0.9% NaCl. Clinical signs of possible intoxication were recorded in the animals during the entire period of observation. Body weight, hematological, biochemical, coagulometric, electrocardiographic parameters were determined, spontaneous daily diuresis was evaluated and clinical urine analysis was performed. Pathological anatomical studies (autopsy, morphometric analysis of internal organs, histological studies) were also conducted. All animals were examined daily to detect mortality or signs of health abnormalities.

3. Results

3.1. Characteristics nanoparticles

As follows from HAADF-STEM images quantum dots are mainly round or triangular in shape, with an average size of 6.7 nm (Fig. S1. A). Atomic rows and individual atomic columns are clearly visible, which indicates QD crystallinity. Individual and mixed EDX maps illustrate the multilevel structure of QDs, whose core is formed by Cd and Se, and the shell consists of S. Visualizing the chemical composition of the shell and antibodies around the particles was difficult because a large amount of carbon present in the sample was dispersed during EDX mapping. Absorption spectroscopy showed that maximum absorption of QDs is below 500 nm (Fig. S1. B). Fluorescence spectrometry showed that fluorescence maximum of QDs is 680 nm (Fig. S1. C). The hydrodynamic particle size in the polymer shell was about 20 nm (Fig. S1. D). In general, size and shape of the QDs under the study are typical for most commercial QDs and those described in the literature [32–42].

3.2. Toxicity at a single IV administration of QDs in mice

Administration of QDs to mice at a dose of 10.0 and 20.0 mg/kg did not result in animal death from toxicity. At the dose of 10 mg/kg and in the control group, the weight of female mice increased uniformly throughout the observation period (30 days) (Fig. S2. A). It should be noted that mice in this group gained body weight more slowly compared to animals in the control group. When administered by 20 mg/kg, mice did not gain weight for 14 days after QDs administration (the weight of mice in this experimental group was 19.70.3 g before QDs administration, and 19.80.5 g on the 14th day after QDs administration). In the next 14 days animals began to gain weight, and on the 30th day after administering QDs the weight of the animals in this experimental group was 21.4 ± 0.9 g (Fig. S2. A). In these groups, water and feed intake slightly changed compared to the control group (Fig. S2 B,C). When 30.0 mg/kg was administered, a delayed death from toxicity was observed in 33% of the mice on days 8 and 9 after administration (Fig. 1) due to adynamy, a pronounced decrease in unconditioned reflexes and body weight by 20% (Fig. S2. A), as well as decreased water and feed consumption (Fig. S2 B,C). After 30 days there was a complete recovery of body weight, water and feed consumption.

At 45.0 and 40.0 mg/kg, two peaks of animal death were observed, immediately after the injection and on day 8–13 after the injection (Fig. 1). Animals that died almost immediately (within 1–3 min) after QDs administration showed pronounced dyspnea and clonic-tonic convulsions (Table S2). In mice that died 8–13 days after the injection,

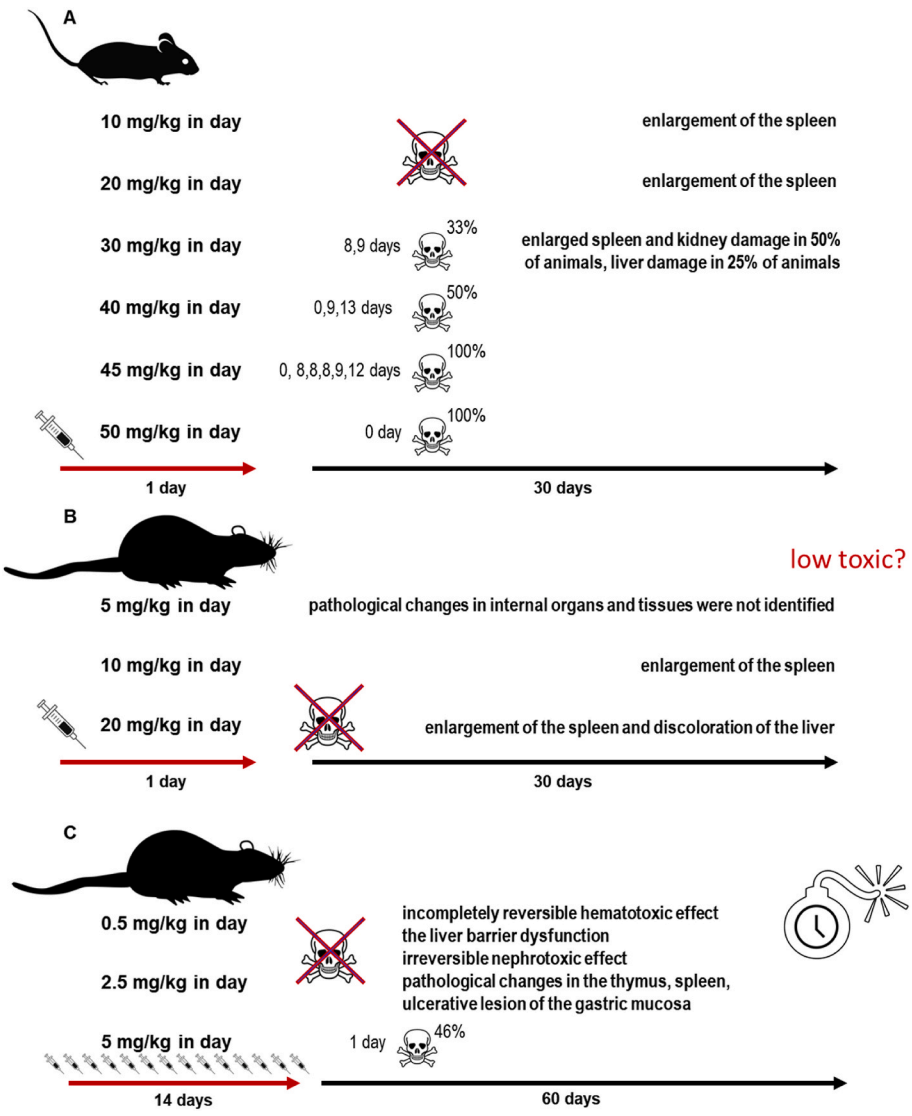

Fig. 1. Pathological changes in animals after administration of QDs. (**A**) A single injection of QDs into mice. When the amount of QDs administration was 10.0 and 20.0 mg/kg at 30 days after autopsy, there was an increase in the spleen in 60% and 100% of animals, respectively. No pathological changes in other organs and tissues of these animals were detected during macroscopic examination. With increasing amount of QDs administration, a dose-dependent lesion of the kidneys and liver was observed. (**B**) A single injection of QDs into mice. When the amount of QDs injection was 10.0 and 20.0 mg/kg 30 days after autopsy, an increase in the spleen was observed in 60% and 100% of animals, respectively. Macroscopic examination revealed no pathological changes in other organs and tissues of these animals. When the dose of QDs administration was increased, a dose-dependent lesion of the kidneys and liver was observed. (**C**) Multiple administration of QDs to rats. Multiple not completely reversible and irreversible lesions of organs and tissues.

adynamia or hypodynamia, decreased unconditioned reflexes (Table S1), and a 25–34% decrease in body weight were observed (Fig. S2. A). Also, these mice had urine with an admixture of blood. When 50.0 mg/kg was administered, all animals died from the toxic effects of QDs within 1–3 min. Severe dyspnea and clonic-tonic seizures were observed in these animals (Table S1). Surviving mice administered with 40.0 and 30.0 mg/kg QDs showed dyspnea and clonic-tonic seizures, as well as hypodynamia, decreased unconditioned reflexes (Table S1), a marked decrease in feed, water consumption, and body weight from days 3–10 after QDs administration, which ranged from 16 to 30% (Fig. S2 A-C).

Autopsies of mice euthanized at 30 days after 10.0 mg/kg injection showed spleen enlargement in 60% of the mice. After administration of 20.0 mg/kg, spleen enlargement was observed in 100% of mice. No pathological changes in other organs and tissues were detected during macroscopic examination. At 30.0 mg/kg we observed enlargement of the spleen and kidneys in 50% of mice; the surface of the kidneys was lumpy, pale brown in color; the boundary between the cortical and cerebral substance was not clearly expressed on the section. In the liver, 1 of 4 mice had multiple small foci of light gray color. No pathological changes in other organs and tissues of these animals were detected during macroscopic examination. Autopsies of mice that died immediately after administration of doses from 30.0 to 50.0 mg/kg revealed pathological changes only in the thoracic cavity: the main vessels were full of blood; the heart was diastolic and significantly enlarged in size (ventricles and atria), large foci of dark maroon color were observed; the lungs were carrot-colored. The pathological changes detected were characteristic of acute pulmonary-cardiovascular failure. Autopsy of mice that died on day 8–13 after administration of QDs from 30.0 to 50.0 mg/kg revealed pathological changes only in the abdominal cavity: the main vessels were full of blood; the spleen increased significantly in size; the liver was pale brown; the kidneys were pale brown; the border between the cortical and brain matter was not marked on the section. The pathological changes detected are characteristic of hepatic-renal insufficiency.

Based on the data obtained, LD50 34.5 (28.3 ÷ 42.1) mg/kg was calculated after a single IV administration of QDs (Table S2).

3.3. Toxicity of single IV administration of QDs to rats

Administration of QDs at doses of 5.0, 10.0, and 20.0 mg/kg did not result in animal death from toxicity. After administration of 5.0 mg/kg there were no external signs of intoxication in the animals: the rats were active, with a pronounced reaction to human, tactile and painful stimuli. After administration of 10.0 and 20.0 mg/kg doses, short reactions (up to 30 s) were observed in rats: pronounced dyspnea, limb tremors and tonic convulsions, as well as adynamia or hypodynamia for 2–3 h after administration.

The weight of the animals at the doses of QDs 5.0, 10.0, and 20.0 mg/kg, as well as in the control group rats, increased uniformly throughout the entire observation period (30 days). The differences between the experimental groups of animals and the control group in body weight for all periods of observation were not statistically reliable (Student's t-criterion) (Fig. S2. D). No differences between the experimental and control groups were found when assessing food and water consumption by the rats (Fig. S2. I and J).

Autopsies of rats at 30 days after administration of 5.0 mg/kg showed no pathological changes in internal organs and tissues. At a dose of 10.0 mg/kg, an enlargement of the spleen was observed in 100% of the animals. No pathological changes in other organs and tissues of these animals were detected during macroscopic examination. At the dose of 20.0 mg/kg an enlargement of the spleen in 100% of animals and the liver was pale yellow in 60% of animals was found.

Thus, intravenous administration of QDs to female rats at the doses studied was satisfactorily tolerated by the animals. There was no death from toxicity.

3.4. Toxicity of multiple IV administration of QDs to rats

Repeated administration of QDs to female rats for 14 days at total doses of 7.0 and 35.0 mg/kg, was satisfactorily tolerated by the animals. When a dose of 70 mg/kg was used on day 1 after QDs withdrawal, animal mortality from toxicity was 46% (Fig. 1). At a dose of 7 mg/kg there were no external signs of intoxication, at 35.0 mg/kg a decrease in motor activity and lethargy were observed for 60 days after QDs withdrawal. The animals did not gain weight during the entire observation period. The total doses of 7 and 35 mg/kg QDs had a moderate and not fully reversible (by the 60th day of observation) hematotoxic effect which manifested itself in a decrease in the total number of red blood cells, hemoglobin, hematocrit value, relative lymphocyte count, an increase in platelet count and relative number of segmented neutrophils (Fig. 2, Tables S3 and S4).

The effect of QDs on liver function (barrier and synthesizing) was assessed by serum biochemical indices and blood plasma coagulometric indices in rats (Fig. 2 and Tables S5 and S6). Hematological studies after 14-fold administration of QDs revealed a progressive dose-dependent delayed and irreversible change in the parameters: the number of erythrocytes, the concentration of hemoglobin, the average

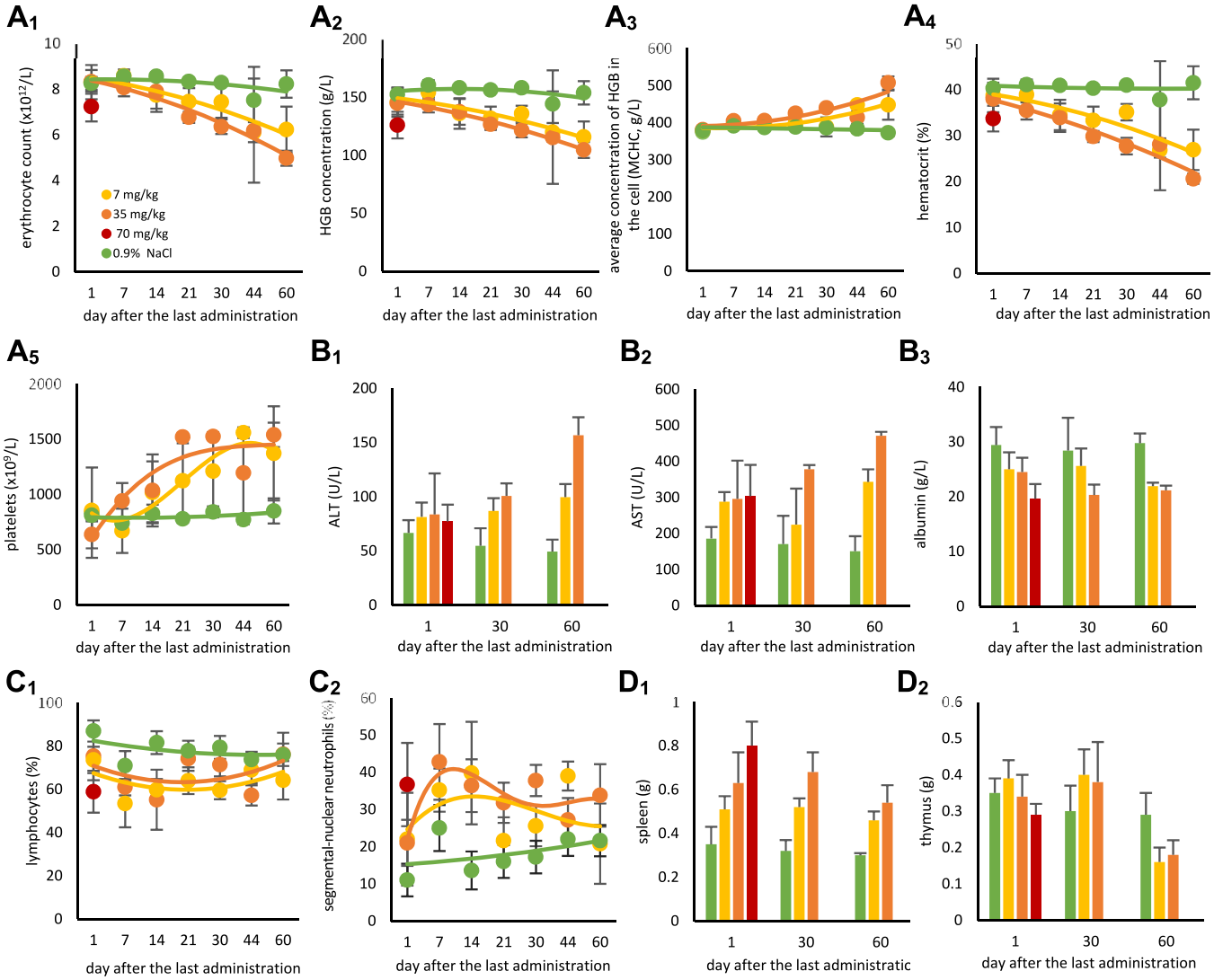

Fig. 2. Hematological studies after multiple administrations of QDs: erythrocyte count, HGB concentration, average concentration of HGB in the cell (A_1 – A_5). **Biochemical indicators of blood serum**: ALT, AST and hemoglobin (B_1–B_3). **Number of lymphocytes and segmented neutrophils** (C_1 and C_2). Weight of organs: spleen D_1 и thymus D_2.

concentration of HGB in the cell, hematocrit, and platelet count (Fig. 2A_1–$2A_5$). Changes were found in serum biochemical indices: ALT, AST and albumin (Fig. 2B1 - 3B3). This indicates irreversible impairment of the barrier function of the liver.

The change found in the leukocyte formula (Table S4) which was a decrease in the number of lymphocytes and a marked increase in the segmented neutrophils is typical for tissue destruction (Fig. 2C1 and 2C2). Administration of QDs in total doses of 7.0 and 35.0 mg/kg for 14 days resulted in irreversible reduction in the absolute weight of the spleen and thymus (Fig. 2D_1 and 2D_2). No change in the absolute weights of the other organs was observed.

In a study of daily diuresis after repeated administration of QDs at a total dose of 7.0 mg/kg, the amount of fluid drunk and excreted by rats in the experimental group and the control group was quite similar (Table S7). At the total dose of 35.0 mg/kg, rats exhibited marked polyuria (daily diuresis was 102%–110% on days 21–60 of observation) (Table S7). Clinical urinalysis revealed significant dose-dependent changes in animals treated with QDs at total doses equal to 7.0 mg/kg and 35.0 mg/kg: decreased urine density (on days 21–60), increased urine pH (alkalinity; on days 21–60), the presence of significant amounts of erythrocytes and leukocytes in the urine of animals (on days 1–60), glucose (on days 60) and ketone bodies (on days 60) (Table S8). Serum glucose levels after repeated administration of QDs at total doses equal to 7.0 mg/kg and 35.0 mg/kg ranged within the physiological norm and did not differ from those obtained in the control animals (Table S5). The amount of total cholesterol in the serum of female rats, after repeated intravenous administration of QDs at total doses of 7.0 mg/kg and 35.0 mg/kg was lower than in animals in the control group. Generally pathological processes in the liver and kidneys cause reduced cholesterol levels (Table S5).

Qualitative and quantitative analysis of electrocardiograms of animals injected with QDs repeatedly in total doses of 7.0 mg/kg (single dose, 0.5 mg/kg) and 35.0 mg/kg (single dose, 2.5 mg/kg) revealed no changes in the indices of cardiac electrical activity throughout the observation period of 60 days. The animals showed no rhythm and conduction abnormalities and no electrocardiographic signs of myocardial damage (Table S9). Using a total dose of QDs of 70 mg/kg (a single dose of 5.0 mg/kg), no changes in the electrical activity of the heart were also observed in the rats on day 1 after the last injection (Table S9).

QDs had no effect on carbohydrate and lipid metabolism, did not lead to clinically significant changes in the main indices characterizing the state of coagulation homeostasis in rats, and had no effect on the central nervous system of animals (based on the analysis of animal behavioral reactions).

Pathological anatomical examination (macroscopic evaluation) and morphometric analysis of the internal organs at the doses of 7.0 and 35.0 mg/kg on the 1st-60th days of observation revealed pathological changes in the thymus (color change and decrease in the organ size), liver (change in the organ relief and its color), kidneys (color and structure change) and spleen (decrease in the organ size). Using QDs at a total dose of 70.0 mg/kg the same changes in the thymus, liver, kidneys and spleen were observed during autopsy, and changes in the stomach (multiple ulcerative lesions of the stomach mucosa) and adrenal glands (increased organ size) were detected.

Histological examination on the first day after administration of a total dose of 35.0 mg/kg QDs revealed multiple emphysematous foci and thickened lung tissue (Fig. S3), there was activation of reticuloendothelial cells in the liver, expressed in the accumulation of stellate endotheliocytes (Kupfer cells) with various sizes of hemosiderin particles (some of these cells had marked signs of destruction) (Fig. S4). In the spleen, mainly in the red pulp and in the sinuses of the lymph nodes, groups of macrophages with the same particles of light brown color were detected (Fig. S5). The observed particles correspond to erythrocyte debris and hemosiderin. In the kidneys, sections of tortuous tubules and Genle loops with signs of destruction and dystrophy of epithelial cells were observed (Fig. S6). In the thyroid gland of female rats pronounced destructive changes were observed (Fig. S7). The detected pathological morphological changes in the thyroid gland, lungs, and liver were reversible (reversibility period - 60 days). By the 60th day of observation the reversibility of pathological morphological changes in the spleen and kidneys was absent (Fig. S8).

Histological examination at a lethal dose of 70.0 mg/kg revealed morphological changes in the thyroid, lung, liver, spleen, kidney, heart, and stomach (Figs. S9–S15). There were marked inflammatory changes in the lungs. In the liver and spleen there was activation of the reticuloendothelial system (RES) cells, which was expressed in the accumulation of light brown particles, representing erythrocyte debris and hemosiderin formed from their hemoglobin, by macrophages of RES. In kidneys we found areas of tortuous tubules and Genle loops with signs of destruction and dystrophy of epithelial cells and their walls, as well as damage to glomerular vascular loops. Vacuolization of cells of glomerular and bundle layers was observed in adrenal glands. Destruction of thyrocytes and complete resorption (absence) of colloid in thyroid gland was detected. In the heart, the rat myocardium showed signs of edema and muscle fiber fragmentation, as well as signs of interstitial inflammation (lymphocytic infiltration). Signs of inflammation and erosion, as well as dystrophic changes in the parietal cells of the fundamental glands were observed in the mucosa of the glandular region of the stomach.

When performing the Perls reaction on paraffin sections of the liver and spleen of rats from all experimental groups on the 1st day after the end of QDs administration in total doses equal to 35.0 and 70.0 mg/kg, the reaction showed not blue but bluish-greenish staining of inclusions of different in size particles in tissue macrophages of the liver and spleen, with the prevalence (severity) of stained cells corresponding to the inclusions of particles in tissue macrophages when stained with hematoxylin and eosin (Figs. S17–S19). The reaction in the rat kidney sections of these groups was expressed only in the presence of single blue rather large particles in the glomerular vessels.

Based on the data obtained, we can assume that RES cells contain both erythrocyte debris and particles - clumps, hemosiderin (iron oxide) formed from the hemoglobin of destroyed erythrocytes. In addition, it can be assumed that in blood nanoparticles interact with the membranes of red blood cells and plasma proteins, causing damage and hemolysis of red blood cells, which are captured by the RES cells.

4. Discussion

We found that QDs had a dose-dependent species-specific toxic effect on animals. At doses greater than 30.0 mg/kg, mice died of spleen, kidney, and liver damage. According to FDA Guidance “Estimating the Maximum Safe Starting Dose in Initial Clinical Trials for Therapeutics in Adult Healthy Volunteers,” in interspecies transfer based on coefficients, the dose in mice is twice as high as the equivalent dose in rats due to the basic metabolic rate from body weight and body surface area. The calculated LD50 value for a single administration in mice was 34.5 mg/kg, so according to FDA guidance for rats this value should be 17.25 mg/kg. Nevertheless, it has been demonstrated that even the 20.0 mg/kg dose did not lead to animal death, no significant toxic effects were detected throughout the experiment. Thus, scientists and regulators developing medical applications based on quantum dots must consider this discordance when transferring their toxicity data from one animal model to another, let alone humans.

Interesting results were obtained in the study of toxicity at repeated administration. Specifically, doses of 0.5 and 2.5 mg/kg administered over 14 days resulted in irreversible organ and tissue damage within 60 days. Using the FDA conversion factors for humans, these doses would be only 80 and 400 mcg/kg. A dose of 5 mg/kg resulted in the death of 46% of rats on the first day after the last injection. The data show that QDs bind to blood components, including erythrocytes, causing their damage and hemolysis. Damaged and destroyed red blood cells are

subsequently taken up by tissue macrophages. First of all, we observed lesions of the organs in which tissue macrophages prevail: spleen, liver, lungs. Obviously, the instant death of animals at high doses of QDs at single and multiple injections is due to hyperhaemolysis, which leads to initiation of autoimmune reactions cascade and hemolytic crisis. QDs take several days to biodegrade in organs. Biodegradation occurs as an immune reaction, leading to the development of inflammation. The released Cd in ionic form is known to accumulate in liver and kidneys. Cd, like other metals, binds to proteins in the bloodstream and can pass freely into the glomerular filtrate. Protein-Cd complexes are then absorbed by the cells of the proximal convoluted tubules, where Cd is released and binds to metallothioneins, resulting in the accumulation of Cd in the cortical substance of the kidneys [43].

The difference in sensitivity of animals with single and multiple administrations of QDs may be due to the use of different strains of rats. It has been shown in Ref. [44] that different strains of rats exhibit varying degrees of intensity and/or nature of response to Cd both locally and systemically.

Nether the whole complex of toxic effects, their difference in different animal species and strains can be explained by the formation of reactive oxygen species (ROS) from nanoparticles, nor the release of Cd during biodegradation of QDs and the formation of ROS. In addition, several systematic reviews suggest that Se or Zn reduces the toxicity of Cd [45,46]. According to EDX maps the S/Se/Cd atom content in nanocrystals is 58 ± 3/17 ± 3/25 ± 4% respectively (Fig. S1). In terms of composition the composition it is impossible to explain how QDs in a polymer shell at high doses can lead to the death of animals almost immediately after administration and why delayed toxic effects are observed.

One of the most likely reasons for different sensitivity to QDs and the presence of delayed toxic effects could be the immune system response and the development of chronic inflammation. Indeed, the results of Perls staining allowed us to detect macrophages with destructed blood components in the tissues after QDs injection. Around these macrophages there were tissue areas with signs of inflammation and dystrophy. The detected pathological changes in the thymus (color change, hypertrophy on day 30 and its pronounced degradation on day 60) also testify in favor of the immunotoxic mechanism. Thymic atrophy leads to cessation or perversion of certain stages of T-cell maturation. Immature T cells enter the periphery and, at the onset of the autoreactive stage, damage the surrounding tissues through the release of a variety of cytokines and adhesive intercellular interactions [47]. A review [48] provides current evidence that components of the immune system are mediators/effectors of Cd tissue toxicity that trigger a cascade of reactions leading to tissue damage. The multiplicity and complexity of such effects are given in Refs. [49–52]. It has been shown that the immune response occurs along the axis of inflamosome activation, proinflammatory cytokine production, inflammation, and tissue apoptosis. However, the underlying mechanism of QDs toxicity remains to be studied.

5. Conclusions

Quantum dots when administrated into the body once have moderate species-specific toxicity. However, repeated administration of quantum dots in a small amount of 0.5 mg/kg of body weight leads to a delayed not completely irreversible hematotoxic effect, delayed irreversible impairment of the liver barrier function, an irreversible nephrotoxic effect, and pathological changes in the thymus, kidneys and spleen. The administration of quantum dots 2.5 mg/kg for 14 days leads to irreversible changes in the lungs, liver, spleen, kidneys and thyroid gland. Observed toxicity is determined by immune responses. This study shows that the toxic effect of quantum dots on a living organism is quite complex and cannot be generalized based on the few assumptions that have been reported previously. This study should push a new round in the research of the toxicity of nanomaterials when they are repeatedly administered into the body.

6. Contributors

Denis Kuznetsov was responsible for drafting the manuscript, analysis and interpretation of data. Dmitriy Krylsky collected and analyzed the data. Sergey Dezhurov contributed analysis of data and manuscript preparation. Alexey Grachev helped perform the analysis with constructive discussions. Valeri Neschisliaev, Ekaterina Orlova and Anastasiia Kuznetsova contributed the conception and design of the current study.

All authors read and approved of the final manuscript. Therefore, all authors had full access to all the data in the study and take responsibility for the integrity and security of the data.

7. Compliance with ethics guidelines

Denis Kuznetsov, Dmitriy Krylsky, Sergey Dezhurov, Alexey Grachev, Valeri Neschisliaev, Ekaterina Orlova, Anastasiia Kuznetsova declare that they have no conflict of interest.

All institutional and national guidelines for the care and use of laboratory animals were followed.

Funding

No Funding

Declaration of competing interest

The authors declare that they have no known competing financial interests or personal relationships that could have appeared to influence the work reported in this paper.

Data availability

The data are presented in the supplementary materials

Acknowledgments

The authors are grateful to Advanced Imaging Core Facility of Skolkovo Institute of Science and Technology for providing data HAADF-STEM image.

Appendix A. Supplementary data

Supplementary data to this article can be found online at https://doi.org/10.1016/j.cbi.2023.110396.

References

[1] C. Hou, W. Yang, H. Kimura, X. Xie, X. Zhang, X. Sun, Z. Yu, X. Yang, Y. Zhang, B. Wang, B.B. Xu, D. Sridhar, H. Algadi, Z. Guo, W. Du, Boosted lithium storage performance by local build-in electric field derived by oxygen vacancies in 3D holey N-doped carbon structure decorated with molybdenum dioxide, J. Mater. Sci. Technol. 142 (2023) 185–195, https://doi.org/10.1016/j.jmst.2022.10.007.

[2] W. Yang, D. Peng, H. Kimura, X. Zhang, X. Sun, R.A. Pashameah, E. Alzahrani, B. Wang, Z. Guo, W. Du, C. Hou, Honeycomb-like nitrogen-doped porous carbon decorated with Co3O4 nanoparticles for superior electrochemical performance pseudo-capacitive lithium storage and supercapacitors, Adv. Composites Hybrid Mater. 5 (4) (2022) 3146–3157, https://doi.org/10.1007/s42114-022-00556-6.

[3] Y. Ma, X. Xie, W. Yang, Z. Yu, X. Sun, Y. Zhang, H. Kimura, C. Hou, Z. Guo, W. Du, Recent advances in transition metal oxides with different dimensions as electrodes for high-performance supercapacitors, Adv. Composites Hybrid Mater. 4 (4) (2021) 906–924, https://doi.org/10.1007/s42114-021-00358-2.

[4] C. Dang, Q. Mu, X. Xie, X. Sun, X. Yang, Y. Zhang, S. Maganti, M. Huang, Q. Jiang, I. Seok, W. Du, C. Hou, Recent progress in cathode catalyst for nonaqueous lithium oxygen batteries: a review, Adv. Composites Hybrid Mater. (2022) 1–21, https://doi.org/10.1007/s42114-022-00500-8.

[5] Q. Mu, R. Liu, H. Kimura, J. Li, H. Jiang, X. Zhang, Z. Yu, X. Sun, H. Algadi, Z. Guo, W. Du, C. Hou, Supramolecular self-assembly synthesis of hemoglobin-like amorphous CoP@ N, P-doped carbon composites enable ultralong stable cycling

under high-current density for lithium-ion battery anodes, Adv. Composites Hybrid Mater. 6 (1) (2023) 23, https://doi.org/10.1007/s42114-022-00607-y.
[6] Y. Ma, Y. Zhang, M. Liu, T. Han, Y. Wang, X. Wang, Improving the performance of quantum dot sensitized solar cells by employing Zn doped CuInS2 quantum dots, 4, Adv. Composites Hybrid Mater. 5 (1) (2022), https://doi.org/10.1007/s42114-021-00324-y, 02-409.
[7] M. Niu, K. Sui, X. Wu, D. Cao, C. Liu, GaAs quantum dot/TiO2 heterojunction for visible-light photocatalytic hydrogen evolution: promotion of oxygen vacancy, Adv. Composites Hybrid Mater. 5 (1) (2022) 450–460, https://doi.org/10.1007/s42114-021-00296-z.
[8] H. Algadi, H. Albargi, A. Umar, M. Shkir, Enhanced photoresponsivity of anatase titanium dioxide (TiO 2)/nitrogen-doped graphene quantum dots (N-GQDs) heterojunction-based photodetector, Adv. Composites Hybrid Mater. 4 (2021) 1354–1366, https://doi.org/10.1007/s42114-021-00355-5.
[9] R. Kottayi, D.K. Maurya, R. Sittaramane, S. Angaiah, Recent developments in metal chalcogenides based quantum dot sensitized solar cells, ES Energy Environ. 18 (2022) 1–40, https://doi.org/10.30919/esee8c754.
[10] F.A. Al-Marhaby, M.S. Al-Ghamdi, A. Zekry, Effect of temperature on the electrical parameters of indium phosphide/aluminum gallium indium phosphide (InP/AlGaInP) quantum dot laser diode with different cavity lengths, Eng. Sci. 1 (2022), https://doi.org/10.30919/es8d647.
[11] D.F. Lauren, Y.C. Chen, J.B. Delehanty, Semiconductor quantum dots for visualization and sensing in neuronal cell systems, Humana, New York, NY, Basic Neurobiol. Techniques (2020) 1–18, https://doi.org/10.1007/978-1-4939-9944-6_1.
[12] H. Lu, Z. Huang, M.S. Martinez, J.C. Johnson, J.M. Luther, M.C. Beard, Transforming energy using quantum dots, Energy Environ. Sci. 13 (5) (2020) 1347–1376, https://doi.org/10.1039/C9EE03930A.
[13] A.M. Wagner, J.M. Knipe, G. Orive, N.A. Peppas, Quantum dots in biomedical applications, Acta Biomater. 94 (2019) 44–63, https://doi.org/10.1016/j.actbio.2019.05.022.
[14] V.G. Reshma, P.V. Mohanan, Quantum dots: applications and safety consequences, J. Lumin. 205 (2019) 287–298, https://doi.org/10.1016/j.jlumin.2018.09.015.
[15] Z. Lv, Y. Wang, J. Chen, J. Wang, Y. Zhou, S. T, Han Semiconductor quantum dots for memories and neuromorphic computing systems, Chem. Rev. 120 (9) (2020) 3941–4006, https://doi.org/10.1021/acs.chemrev.9b00730.
[16] F.P. García de Arquer, D.V. Talapin, V.I. Klimov, Y. Arakawa, Semiconductor quantum dots: technological progress and future challenges, Science 373 (2021) 6555, https://doi.org/10.1126/science.aaz8541, eaaz8541.
[17] Y. Yan, J. Gong, J. Chen, Z. Zeng, W. Huang, K. Pu, J. Liu, P. Chen, Recent advances on graphene quantum dots: from chemistry and physics to applications, Adv. Mater. 31 (21) (2019), 1808283, https://doi.org/10.1002/adma.201808283.
[18] L. Wang, W. Li, L. Yin, Y. Liu, H. Guo, J. Lai, Y. Han, G. Li, M. Li, J. Zhang, R. Vajitai, P.M. Ajayan, M. Wu, Full-color fluorescent carbon quantum dots, Sci. Adv. 6 (40) (2020), eabb6772, https://doi.org/10.1126/sciadv.abb6772.
[19] J. Lin, Y. Lu, X. Li, F. Huang, C. Yang, M. Liu, N. Jiang, D. Chen, Perovskite quantum dots glasses based backlit displays, ACS Energy Lett. 6 (2) (2021) 519–528, https://doi.org/10.1021/acsenergylett.0c02561.
[20] U. Abd Rani, L.Y. Ng, C.Y. Ng, E. Mahmoudi, A review of carbon quantum dots and their applications in wastewater treatment, Adv. Colloid Interface Sci. 278 (2020), 102124, https://doi.org/10.1016/j.cis.2020.102124.
[21] S. Tajik, Z. Dourandish, K. Zhang, H. Beitollahi, Q. Van Le, H.W. Jang, M. Shokouhimehr, Carbon and graphene quantum dots: a review on syntheses, characterization, biological and sensing applications for neurotransmitter determination, RSC Adv. 10 (26) (2020) 15406–15429, https://doi.org/10.1039/D0RA00799D.
[22] S. Xu, L. Xiaojing, S. Xinyue, C. Wei, L. Honggui, Pig lung fibrosis is active in the subacute CdCl2 exposure model and exerts cumulative toxicity through the M1/M2 imbalance, Ecotoxicol. Environ. Saf. 225 (2021), 112757, https://doi.org/10.1016/j.ecoenv.2021.112757.
[23] M.D. Villalva, V. Agarwal, M. Ulanova, P.S. Sachdev, Nady Braidy, Quantum dots as a theranostic approach in Alzheimer's disease: a systematic review, Nanomedicine 16 (18) (2021) 1595–1611, https://doi.org/10.2217/nnm-2021-0104.
[24] D. Mo, L. Hu, G. Zeng, G. Chen, J. Wan, Z. Yu, Z. Huang, K. He, C. Zhang, M. Cheng, Cadmium-containing quantum dots: properties, applications, and toxicity, Appl. Microbiol. Biotechnol. 101 (7) (2017) 2713–2733, https://doi.org/10.1007/s00253-017-8140-9.
[25] N. Li, F. Lei, D. Xu, Y. Li, J. Liu, Y. Shi, One-step synthesis of N, P Co-doped orange carbon quantum dots with novel optical properties for bio-imaging, Opt. Mater. 111 (2021), 110618, https://doi.org/10.1016/j.optmat.2020.110618.
[26] A.M. Saeboe, A.Y. Nikiforov, R. Toufanian, J.C. Kays, M. Chern, J.P. Casas, K. Han, A. Piryatinski, D. Jones, A.M. Dennis, Extending the near-infrared emission range of indium phosphide quantum dots for multiplexed in vivo imaging, Nano Lett. 21 (7) (2021) 3271–3279, https://doi.org/10.1021/acs.nanolett.1c00600.
[27] X. Zhang, X. Wu, X. Liu, G. Chen, Y. Wang, J. Bao, X. Xu, X. Liu, Q. Zhang, K. Yu, W. Wei, J. Liu, J. Xu, H. Jiang, P. Wang, X. Wang, Heterostructural CsPbX3-PbS (X= Cl, Br, I) quantum dots with tunable Vis–NIR dual emission, J. Am. Chem. Soc. 142 (9) (2020) 4464–4471, https://doi.org/10.1021/jacs.9b13681.
[28] Q. Wang, W.Q. Chen, X.Y. Liu, Y. Liu, F.L. Jiang, Thermodynamic implications and time evolution of the interactions of near-infrared PbS quantum dots with human serum albumin, ACS Omega 6 (8) (2021) 5569–5581, https://doi.org/10.1021/acsomega.0c05974.
[29] D.A. Hanifi, N.D. Bronstein, B.A. Koscher, Z. Nett, J. Swabeck, K. Takano, A. M. Schwartzberg, L. Maserati, K. Vandewal, Y. Burgt, A. Salleo, A. Alivisator, Redefining near-unity luminescence in quantum dots with photothermal threshold quantum yield, Science 363 (6432) (2019) 1199–1202, https://doi.org/10.1126/science.aat3803.
[30] H. Xiaoquan, M. Tang, Research advance on cell imaging and cytotoxicity of different types of quantum Dots, J. Appl. Toxicol. 41 (3) (2021) 342–361, https://doi.org/10.1002/jat.4083.
[31] L. Na, M. Tang, Toxicity of different types of quantum dots to mammalian cells in vitro: an update review, J. Hazard Mater. 399 (2020), 122606, https://doi.org/10.1016/j.jhazmat.2020.122606.
[32] X. Xiang, C. Wu, B.R. Zhang, T. Gao, J. Zhao, L. Ma, F. Jianga, Y. Liu, The relationship between the length of surface ligand and effects of CdTe quantum dots on the physiological functions of isolated mitochondria, Chemosphere 184 (2017) 1108–1116, https://doi.org/10.1016/j.chemosphere.2017.06.091.
[33] V.K. Sharma, T.J. McDonald, M. Sohn, G.A.K. Anquandah, M. Pettine, R. Zboril, Assessment of toxicity of selenium and cadmium selenium quantum dots: a review, Chemosphere 188 (2017) 403–413, https://doi.org/10.1016/j.chemosphere.2017.08.130.
[34] E. Yaghini, H. Turner, A. Pilling, I. Naasani, A.J. MacRobert, In vivo biodistribution and toxicology studies of cadmium-free indium-based quantum dot nanoparticles in a rat model, Nanomed. Nanotechnol. Biol. Med. 14 (8) (2018) 2644–2655, https://doi.org/10.1016/j.nano.2018.07.009.
[35] G. Chen, Y. Zhang, D. Huang, Y. Liu, C. Li, Q. Wang, Long-term chemical biotransformation and pathways of Cd-based quantum dots in mice, Nano Today 44 (2022), 101504, https://doi.org/10.1016/j.nantod.2022.101504.
[36] G. Lin, Q. Ouyang, R. Hu, Z. Ding, J. Tian, F. Yin, In vivo toxicity assessment of non-cadmium quantum dots in BALB/c mice, Nanomed. Nanotechnol. Biol. Med. 11 (2) (2015) 341–350, https://doi.org/10.1016/j.nano.2014.10.002.
[37] L. Hu, H. Zhong, Z. He, Toxicity evaluation of cadmium-containing quantum dots: a review of optimizing physicochemical properties to diminish toxicity, Colloids Surf. B Biointerfaces (2021), 111609, https://doi.org/10.1016/j.colsurfb.2021.111609.
[38] L. Ye, K.T. Yong, L. Liu, I. Roy, R. Hu, J. Zha, H. Cai, W. Law, J. Liu, K. Wang, J. Liu, Y. Liu, Y. Hu, X. Zhang, M.T. Swihart, P.N. Prasad, A pilot study in non-human primates shows no adverse response to intravenous injection of quantum dots, Nat. Nanotechnol. 7 (7) (2020) 431–455, https://doi.org/10.1201/9780429399039.
[39] V.G. Reshma, K.S. Rajeev, K. Manoj, P.V. Mohanan, Water dispersible ZnSe/ZnS quantum dots: assessment of cellular integration, toxicity and bio-distribution, J. Photochem. Photobiol. B Biol. 212 (2020), 112019, https://doi.org/10.1016/j.jphotobiol.2020.112019.
[40] K.C. Nguyen, P. Rippstein, A.F. Tayabali, W.G. Willmore, Mitochondrial toxicity of cadmium telluride quantum dot nanoparticles in mammalian hepatocytes, Toxicol. Sci. 146 (1) (2015) 31–42, https://doi.org/10.1093/toxsci/kfv068.
[41] B.B. Manshian, S.J. Soenen, A. Al-Ali, A. Brown, N. Hondow, J. Wills, G.J. S. Jenkins, S.H. Doak, Cell type-dependent changes in CdSe/ZnS quantum dot uptake and toxic endpoints, Toxicol. Sci. 144 (2) (2015) 246–258, https://doi.org/10.1093/toxsci/kfv002.
[42] L. Zhao, W. Zong, H. Zhang, R. Liu, Kidney toxicity and response of selenium containing protein-glutathione peroxidase (Gpx3) to CdTe QDs on different levels, Toxicol. Sci. 168 (1) (2019) 201–208, https://doi.org/10.1093/toxsci/kfy297.
[43] S.V. Dezhurov, A.Yu Trifonov, M.V. Lovygin, A.V. Rybakova, D.V. Krylsky, Synthesis of highly photostable NIR-emitting quantum dots CdTeSe/CdS/CdZnS/ZnS, Nanotechnol Russ 11 (2016) 337–343, https://doi.org/10.1134/S199507801603006X.
[44] A.E. Egger, G. Grabmann, C. Gollmann-Tepeköylü, E.J. Pechriggl, C. Artner, A. Türkcan, C.G. Hartinger, H. Fritsch, B.K. Keppler, E. Brenner, M. Grimm, B. Messner, D. Bernhard, Chemical imaging and assessment of cadmium distribution in the human body, Metallomics 11 (12) (2019) 2010–2019, https://doi.org/10.1039/c9mt00178f.
[45] M. Ninkov, A.P. Aleksandrov, I. Mirkov, J. Demenesku, D. Mileusnic, S. Jovanovic Stojanov, N. Golic, M. Tolinacki, L. Zolotarevski, D. Kataranovski, I. Brceski, M. Kataranovski, Strain differences in toxicity of oral cadmium intake in rats, Food Chem. Toxicol. 96 (2016) 11–23, https://doi.org/10.1016/j.fct.2016.07.021.
[46] M. Nordberg, G.F. Nordberg, Metallothionein and cadmium toxicology - historical review and commentary, Biomolecules 12 (3) (2022) 360, https://doi.org/10.3390/biom12030360.
[47] I. Zwolak, The role of selenium in arsenic and cadmium toxicity: an updated review of scientific literature, Biol. Trace Elem. Res. 193 (1) (2020) 44–63, https://doi.org/10.1007/s12011-019-01691-w.
[48] C. Hu, K. Zhang, F. Jiang, H. Wang, Q. Shao, Epigenetic modifications in thymic epithelial cells: an evolutionary perspective for thymus atrophy, Clin. Epigenet. 13 (1) (2021) 1–16, https://doi.org/10.1186/s13148-021-01197-0.
[49] I. Mirkov, A.P. Aleksandrov, M. Ninkov, D. Tucovic, J. Kulas, M. Zeljkovic, D. Popovic, M. Kataranovski, Immunotoxicology of cadmium: cells of the immune system as targets and effectors of cadmium toxicity, Food Chem. Toxicol. 149 (2021), 112026, https://doi.org/10.1016/j.fct.2021.112026.
[50] X. Li, H. Li, D. Cai, P. Li, J. Jin, X. Jiang, Z. Li, L. Tian, G. Chen, J. Sun, W. Bai, Chronic oral exposure to cadmium causes liver inflammation by NLRP3 inflammasome activation in pubertal mice, Food Chem. Toxicol. 148 (2021), 111944, https://doi.org/10.1016/j.fct.2020.111944.
[51] J. Ge, K. Guo, C. Zhang, M. Talukder, M.W. Lv, J.Y. Li, J.L. Li, Comparison of nanoparticle-selenium, selenium-enriched yeast and sodium selenite on the alleviation of cadmium-induced inflammation via NF-kB/IκB pathway in heart, Sci. Total Environ. 773 (2021), 145442, https://doi.org/10.1016/j.scitotenv.2021.145442.
[52] N. Hossein-Khannazer, G. Azizi, S. Eslami, H.A. Mohammed, F. Fayyaz, R. Hosseinzadeh, A.B. Usman, A.N. Kamali, H. Mohammadi, F. Jadidi-Niaragh, E. Dehghanifard, M. Noorisepehr, The effects of cadmium exposure in the

induction of inflammation, Immunopharmacol. Immunotoxicol. 42 (1) (2020) 1–8, https://doi.org/10.1080/08923973.2019.1697284.